Entropy **2014**, *16*, 5211-5222; doi:10.3390/e16105211

OPEN ACCESS

entropy

ISSN 1099-4300

www.mdpi.com/journal/entropy

Article

A Further Indication of the Self-Ordering Capacity of Water Via the Droplet Evaporation Method

Igor Jerman [†,*] **and Petra Ratajc** [†]

Bion, Institute for Biolectromagnetics and New Biology d.o.o., Stegne 21, 1000 Ljubljana, Slovenia; E-Mail: petra.ratajc@bion.si

† Both authors contributed equally to this work.

* Author to whom correspondence should be addressed; E-Mail: igor.jerman@bion.si; Tel.: +386-1-5131-146; Fax: +386-1-5131-147.

External Editor: Gerald Pollack

Received: 28 July 2014; in revised form: 26 September 2014 / Accepted: 30 September 2014 / Published: 7 October 2014

Abstract: The droplet evaporation method (DEM) is increasingly used for assessing various characteristics of water. In our research we tried to use DEM to detect a possible self-ordering capability of (spring) water that would be similar to the already found and described autothixotropic phenomenon, namely increasing order of non-distilled water subject to aging. The output of DEM is a droplet remnant pattern (DRP). For analysis of DRP images we used a specially developed computer program that does the frequency distribution analysis of certain parameters of the images. The results of experiments demonstrated statistically significant differences in both aging of water as well as in the glass exposed surface/volume ratio of the aged water. The most important result supporting the self-ordering character of water was found in an increasing dependence between two analyzed parameters: distance and frequency, at the peak frequency. As the result concerns mostly aging and shows increasing order it further corroborates other findings concerning increasing order by aging. Such further confirmation of self-ordering capacity of water is not important only for physical chemistry, but also for biology.

Keywords: water; droplet evaporation method; droplet remnant patterns; supramolecular order; incubation time; surface/volume ratio

---

1. Introduction

The supramolecular order of water, be it water clusters [1–3], coherent domains [4], exclusion zone water [5] and other similar phenomena is still controversial, despite various theoretical considerations and positive results obtained from numerous different experiments. Among the many methods that are being used in this research, the droplet evaporation method (DEM) used with water or some other solvent or liquid, is a very promising—though not a simple—one. It implies the evaluation of certain features of evaporated water drops monitored by dark field microscopy. This method has several modalities and applications. For example, it can be used to monitor diseases via blood drops evaporation [6], for salt induced protein self-assembly research [7], *etc.* The method can be highly sensitive to even the most minuscule concentrations of substances that water was exposed to prior to evaporation, as shown by the fact that one can even differentiate between various wheat cultivars [8].

Despite being a non-linear and highly complex process, the evaporation of water droplets also found physical descriptions in terms of mathematical models, where the formation of droplet remnant pattern (DRP) is described in terms of the so-called self pinning of colloidal drops theory [9,10]. It seems that a complex and dynamic process is taking place during evaporation, providing an immensely rich variety of DRPs that are partially defined by the concentration of colloidal particles, their average size, velocity of evaporation, *etc.* [11,12]. Consequently, certain properties of DRP are strongly influenced by the material composition of the solution to-be-evaporated (like viscosity, composition, total dissolved solids – TDS) and by certain ambient parameters as for example temperature, moisture, pressure *etc.* [12,13].

Furthermore, it seems that the properties of DRP are also influenced by the subtle physical characteristics of solution. Thus, DEM has also been used to research the still controversial special characteristics of ultra-high diluted aqueous solutions [14]. It proved capable of demonstrating differences in subtle influences of a ultra-high dilution (around 10^{-47} M, practically "pure" water) of As_2O_3 (UDH As) on common wheat seeds. DRP originating from the UHD As with immersed wheat seeds demonstrated more complex and symmetrical formations than the control (DRP from water with immersed wheat seeds). This method is therefore capable of transferring certain not yet fully understood or generally accepted subtle physical characteristics [15–17] of the solution to the remnant patterns after drop evaporation.

It is therefore highly probable that some stable supramolecular water structures, such as the ones from the theory of exclusion-zone (EZ) water [18] or those known as the autothixotropic phenomenon [19,20], can also be transferred and "coded" into the droplets. Such proof of transfer of a hidden order from the solution to the DRPs could further strengthen the still controversial theories and empirical findings concerning the evidence of a high level supramolecular order in liquid water. We know that ordinary physics and chemistry consider water to be more or less subject only to Brownian motion, which represents the negation of any true order or long range correlations.

In our previous experiments with aqueous solutions of $NaHCO_3$ [21], we found higher electrical conductivity in the aged solutions than in the chemically analogous fresh (one day old) ones. The phenomenon was discovered in distilled water or water solutions left undisturbed for longer periods of time (~1 year). Most likely, the dissolved ions, as well as the contact with hydrophilic surfaces, played an essential role. In our research, we found that the higher conductivity was proportional to the higher

surface *vs.* volume ratio. This finding corroborated those of Vybiral and Voráček [19] concerning the autothixotropic nature of water, when the latter is subject to aging with minimal disturbance.

Because of the length (duration) of exposure to glass-surfaces as well as the size of these surfaces proved to be important, we designed a new set of experiments using DEM. We exposed spring water of known quality and characteristics to various glass surfaces and monitored the DRPs through a specifically designed computer program. The decision to use spring water stemmed partially from the conclusion found in the work of Vybiral [22] that the autothixotropic phenomenon depends on ions dissolved in water, which was further elaborated by Yakhno [23] and partially from our experience with such water. From our experience with DEM on one hand and the already known self-ordering capacities of water solutions on the other [21], our working hypothesis was that both aging and surface contact would result in some sort of higher order of the DRPs. We therefore designed a series of experiments that were intended to examine characteristics of water (via DRPs) one hour (t_h), one day (t_d), one week (t_w) and one month (t_m) after filling the vials with spring water of known origin and with well researched characteristics of its DRPs. For simultaneous testing of different surface/volume (S/V) ratios one third of the vials were filled only with water (basic surface, S_0), another third with large glass beads (larger surface area, S_1) and the final third with smaller beads (yielding the largest surface area, S_2)—for details see Experimental Section.

2. Results and Discussion

The first result of the DEM is a representation of DRP. Certain types of water provide relatively similar images, while others show more variety. The DRPs of the water used in the present study have typical forms, and are bluish in color—often revealing a "black-hole"-like center. Figure 1 shows representations of our 12 different treatments (three S/V-ratios as a time-series of four separate sampling and drying events (four incubation time points)). Visual assessment of the DRPs involves an examination of the border line, the ring region and the central region. Distinctness of the border line is prominent in all treatments. Difference in thickness of the ring region and the formation of additional structures can be observed at t_d, t_w and t_m. After the last incubation time point (t_m), the DRPs of all three S/V-ratios display greater diversity. The majority of the central regions remains without mineral deposits or any special structures, the mechanism of which is well described in Deegan *et al.* [11]. Since the images vary a lot, the parameters and algorithms (computer programs) have to be selected very carefully, in order to enable us to glance at some of the more orderly structures and dependences (significant correlations).

The DRP images are usually highly complex and can be analyzed in numerous ways. Some authors look for the differences in contrast, fractal dimension [8,24], while others find the symmetry of DRP images to be an important parameter for the measuring of differences using DEM [14,25]. A possible way to group the ways of pattern evaluation is also the one used in [26] which distinguishes between the sizing parameters and shape-descriptors. Of course, such analysis can only reveal one subset of DRP characteristics, meaning that even though it is sophisticated, it is still subject to limitations. The first limitation in our investigation was the fact that our special software computed and yielded only the frequency distribution of distances between illuminated pixels. A further limitation resides in the fact that we used only one specific point of the frequency graphs, namely the maximal frequency.

There are many other possible characteristics of the frequency graphs that could be abstracted for further analysis, but we concluded that they would all be more arbitrary than the one we selected. And besides, d_{max} proved itself as a relatively robust parameter.

Figure 1. Typical DRP images of the chosen spring water. Images depict treatments with three different surface sizes—S_j (S_0—no glass beads, S_1—filled with 10 mm glass beads, S_2—filled with 3 mm glass beads; see Table 2) at four different times—t_i (t_0—after 1 hour, t_d—after 1 day, t_w—after 1 week, t_m—after 1 month). Dark-field microscopy; 40× magnification.

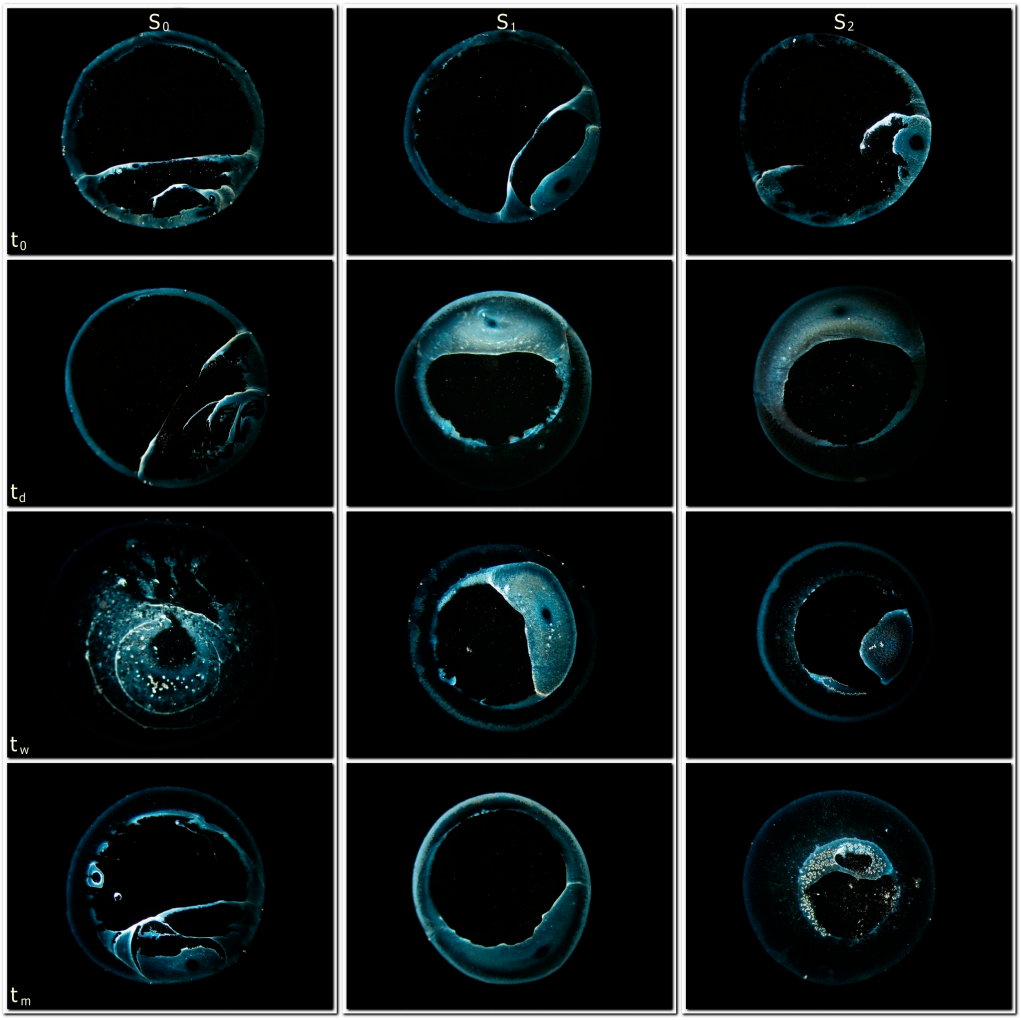

We assume that some more advanced analysis with a more sophisticated method of research—for instance performing Fourier analysis of the images—would yield more refined and richer results, and would provide a deeper insight into the orderliness behind DRPs. However, even with the relatively simple software available and with only one cardinal point per graph (see Figure 5), we obtained statistically significant results that at least roughly corresponded to our working hypothesis. Even though we took only one point per graph, taking many such graphs together enabled us to monitor three different parameters with their statistical characteristics: D_{max}, FR_{max} (see Experimental Section) and the dependence between the two (involving d_{max} and fr_{max}), while also taking into account the four points of incubation and the three different S/V ratios.

As to the distance itself, the statistical analysis shows a significant difference between S_0 and S_1 on the one hand and S_2 on the other (one-way ANOVA; $p = 0.0077$, see Figure 2A). Therefore it seems that the S/V-ratio had an effect on the water that was then further transferred to the structure of the droplet remnants themselves—namely, D_{max} (through all incubation times) of S_2 was significantly smaller than the other two. The direct physical interpretation of the results in terms of the processes behind these effects would be too far-fetched, at least at the present state of research.

On the other hand, we could see no significant effect of the water incubation time (t_i) (one-way ANOVA, $p = 0.2928$) and even if we neglected this statistical evaluation, we see no clear trend, since the smallest D_{max} was achieved after 1 day of incubation and the highest after 1 week (see Figure 2B). Perhaps this independence of D_{max} (and also FR_{max}, see Figure 2D) from time is a sign that our analysis was insensitive to a possible silicate or Na^+ dissolution (even if very minuscule) from the glass into the water, since it is not only a function of S, but also of time.

Figure 2. Effect of surface (S_j—see Table 2 for explanation) and time of incubation (t_i—see Figure 1 for explanation) on D_{max} (A and B) and FR_{max} (C and D). Averages ± standard errors are presented. Different upper-case letters on (A) indicate significant differences according to Duncan's multiple range test ($p < 0.05$). Different letters over the bars on (C) and (D) indicate significant differences in medians according to Kruskal–Wallis test ($p < 0.05$).

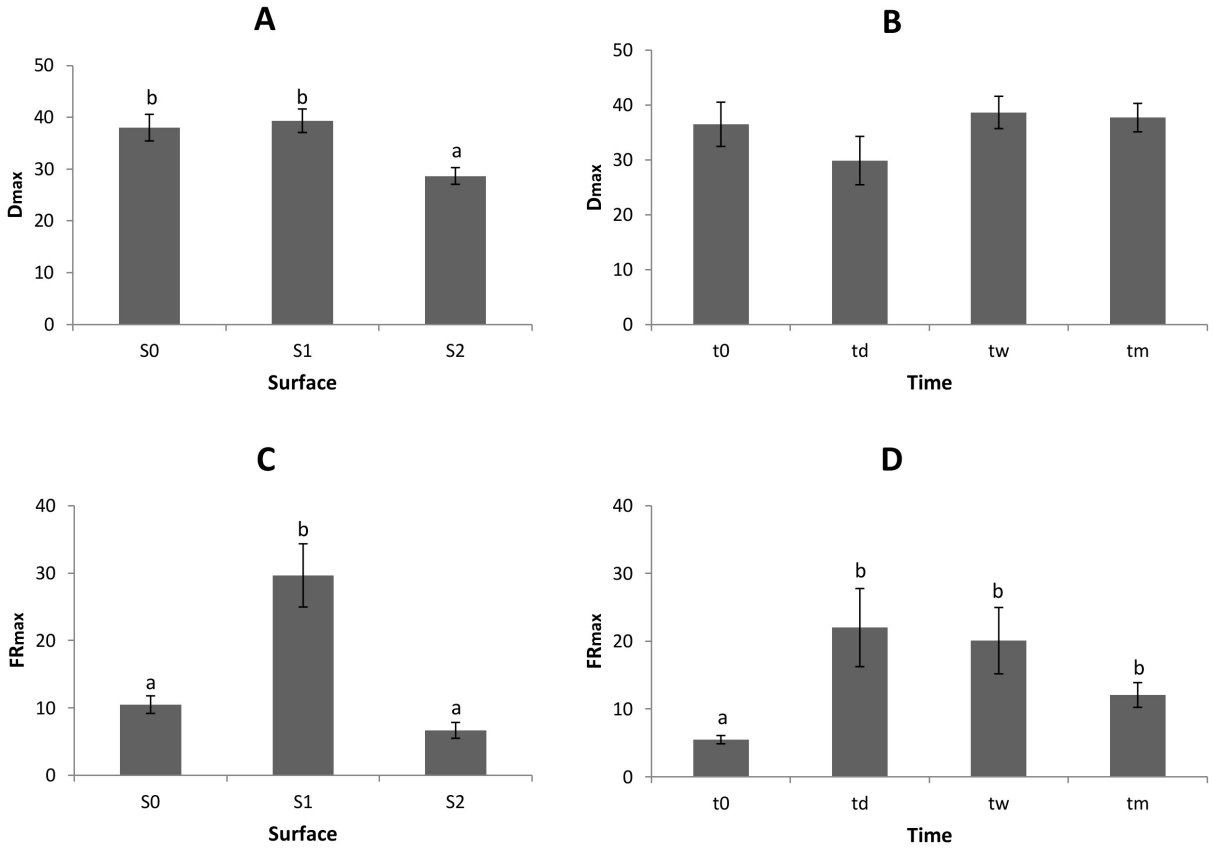

The analogous results concerning FR_{max} also yielded statistically significant results in the S_j domain, as revealed by Kruskal–Wallis test of medians ($p = 0.001$, see Figure 2C). A significant difference was observed between S_0 and S_1 on one hand as well as between S_1 and S_2 on the other.

Surface S_1 demonstrated a much higher average frequency than either S_0 or S_2. Even though the result seems to be a bit misleading, it clearly delineates S_1 from S_2, with S_0 in between (closer to S_2). It also seems that a high S (S_1) determines a high D_{max} and a high FR_{max}, while a very high S (S_2) influences the evaporation in the direction of very small distances as well as very small frequencies (Figure 3).

Figure 3. Differences of average maximal frequency points in S_j domain (see Table 2) in dependence from D_{max}. Averages in both dimensions ± standard error are presented.

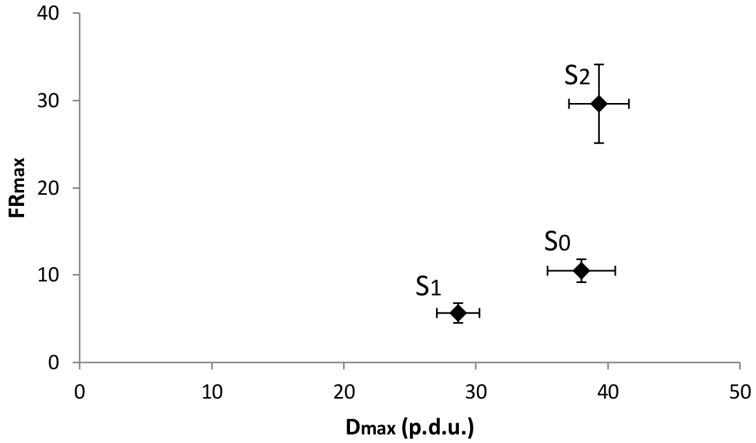

For incubation time (t_i) FR_{max} results show a significant difference between the starting point (t_0) and the other three points (t_d, t_w, t_m) (Kruskal–Wallis test, $p = 0.0166$) (see Figure 2D). It seems that shortly after the start of the incubation certain processes began that resulted in a high frequency, while afterwards the frequency shows a trend towards the starting level ($FR_{max}(t_d) > FR_{max}(t_w) > FR_{max}(t_m) > FR_{max}(t_0)$).

Taking all these results into account, we can conclude that the DRPs demonstrate differences in either S_j or t_i domain via at least one parameter. But there is still no clear evidence as to whether some hidden order comes to the fore through time or via S/V-ratio. To clarify this important issue, we calculated the dependence between the two parameters: d_{max} and fr_{max} with linear regression analysis. We assumed that the dependence is based on two factors: the correlation between the two parameters and the significance of the given linear regression line.

We did not find any dependence in the S_j domain, but we discovered an increasing dependence in the t_i domain, as demonstrated in Figure 4 and Table 1, achieving relatively high correlation and high significance of the linear regression line at t_m. This dependence shows an increase in order throughout the incubation time. In other words, a certain relation is gradually established during incubation, so that when d_{max} increases, so does the corresponding fr_{max}. However, considering that the results show no big difference between t_m and t_w, we could conclude that the dependence (order) was formed somewhere before or at least at one week incubation time and then remained more or less constant.

Is this all that can be said about the DRP images? No, because, as previously stated, there are many other analyses of the images possible, which could demonstrate other dependencies and other features of incubation time as well as the S/V-ratio. Even our selection of typical images (see Figure 1) displays some general differences between the variously treated waters (different S_j or/and t_i) that are mostly neglected by our present algorithm.

Figure 4. Linear regression analysis between d_{max} and fr_{max} at t_0 (A), t_d (B), t_w (C) and t_m (D) (for explanation of different t_i see Figure 1 or Section 3.2).

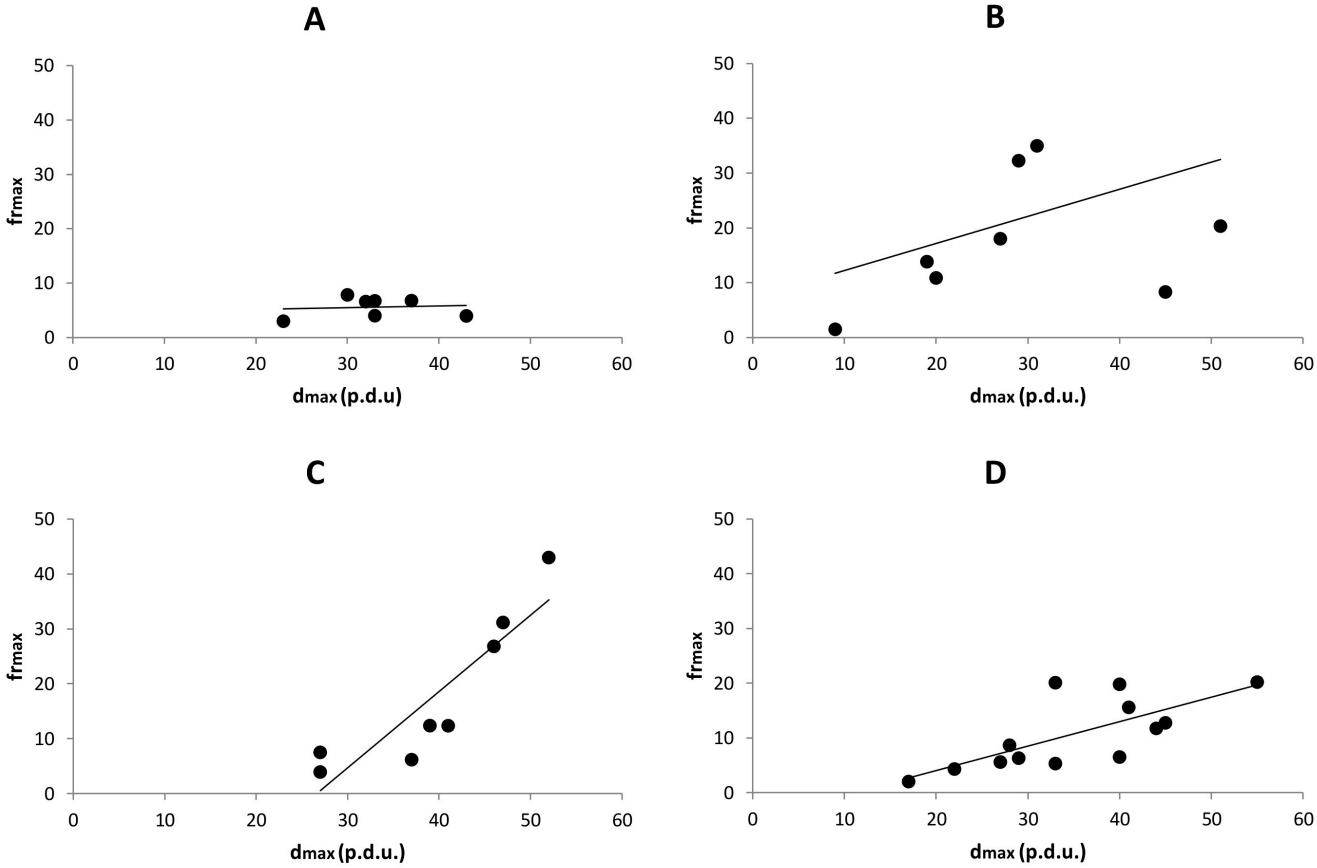

Table 1. Linear regression parameters between d_{max} and fr_{max} for all four sampling incubation points.

Time point	N	Intercept	Slope	R^2	$p < 0.05$
t_0	7	4.565	0.030	0.090	0.8341
t_d	8	7.207	0.495	0.379	0.3142
t_w	8	−36.880	1.387	0.890	0.0027
t_m	11	−6.278	0.462	0.829	0.0008

3. Experimental Section

3.1. Droplets Evaporation Method

The method of monitoring dried water drops by dark field microscopy was discovered in the previous century by German artist Ruth Kübler [27] and further developed by Kröplin, Hein [28], Heusel [29] and Schröcker [30,31]. The method consists of creating drops of different solutions on clean microscope slides and drying them under defined conditions. Dry residues are then observed under the microscope and the anomalously dried drops (evidently non-circular form, ripped up or interrupted edges) or drops with fibers or dust-like particles (occasionally stemming from previous cleaning of slides) incorporated in dry residues are eliminated from further analysis. Properly dried drops with no additional artifacts are photographed and analyzed by visual assessment and software.

3.2. Experimental Protocol

Bottled spring water from a well known source (Spring Living water from the Tunjice Natural Health Resort; Na—1.7 mg/L, K—0.46 mg/L, Mg—1.6 mg/L, Ca—40.2 mg/L, I—0.05 mg/L, HCO_3—119 mg/L, SiO_2—9.2 mg/L, dry residue 180 °C—137 mg/L, pH—7.6; Analysis: The Institute of Public Health Kranj, 2005) was incubated in 20 mL transparent glass bottles (Wheaton, Millville, NJ, USA). The surface of water in contact with glass was increased using glass beads (3 mm or 10 mm, Assistent, Glaswarenfabrik Karl Hecht KG, Sondheim, Germany). The sampled volume of spring water incubated in the bottles without glass beads was 20 mL, and 10 mL in the bottles filled with glass beads. During the experiment, all bottles were tightly sealed, stored in the dark and put to rest, at room temperature. We disregarded the potential effects of impurities released from the glass of the bottles.

Structural changes in water were evaluated using the evaporation method after one hour (t_0), one day (t_d), one week (t_w) and one month (t_m) of incubation. From each bottle 14–16 water drops (3 μL each) were placed on clean microscope slides (Assistant) with an automatic pipette and then dried under laboratory conditions (temperature 22–25 °C, moisture 44–48%.). Microscopic slides were previously cleaned with 70% ethanol and rinsed with distilled water. The patterns of individual droplet residues were observed under dark field microscope (Euromex ME 2665, Euromex, Arnhem, The Netherlands) at 40× magnification after approximately 1 hour of evaporation. Properly dried drops were photographed by a digital camera (2048 × 1536 resolution) and analyzed.

3.3. Experimental Design

We studied the influence of three different surface sizes (S_j) and four different incubation times (t_i) at maximum distance (d_{max}) and maximum frequency (fr_{max}). Three different surface sizes (S_j) were designated as S_0, S_1, S_2 (see Table 2). As previously stated, water drops were prepared at 4 different times. Time t_0 is considered as a starting point, where the water was still considerably disturbed, at least while filling the bottles. All subsequent procedures (at t_d, t_w and t_m) left the water almost undisturbed. All three S_j variants were prepared at all four times. Experiments were performed in triplicates, *i.e.*, three parallel bottles were prepared (A, B and C) and analyzed for each set of samples S_i. Drops from each bottle were placed on one microscope slide, except at t_m where drops were placed on three different slides from each A parallel (triplicate of A) and on one slide from the parallels B and C. This is the reason that there are more data for the t_m than for other t_i.

Table 2. Properties of different S_j with or without additional glass beads

Property	S_0	S_1	S_2
Volume of water (ml)	20	10	10
Beads size (mm)	/	10	3
Glass surface (cm^2)	35.207	98.007	270.327
S/V-ratio (cm^2/cm^3)	1.76	9.80	27.03

3.4. Evaluation of Droplet Remnant Patterns

DRP images were analyzed with a computer software developed especially for our DEM. The program divides the diameter size into 200 equal intervals (designated as p.d.u.-s, procedure defined units). Then the algorithm of the program performs a frequency analysis of all distances between all illumined pixels (representing dry residues within the droplet remnants perimeter). Therefore all the distances between pixels of a DRP image are arranged into one of 200 possible intervals. The frequency distribution analysis roughly captures some structural features of a DRP.

Many different features of the frequency analysis can be used to seek some characteristics or a hidden order behind the DRPs. In this study, we used a clearly defined cardinal point of the average frequency distribution graph of all correctly formed drops form one slide (14–16 drops), namely, its peak and the corresponding maximal frequency (designated as p_{max}) (see Figure 5).

Figure 5. An example of an average frequency distribution graph for all drops from one slide at a chosen time. We defined p_{max} through the relation between d_{max} on x-axis and fr_{max} on y-axis.

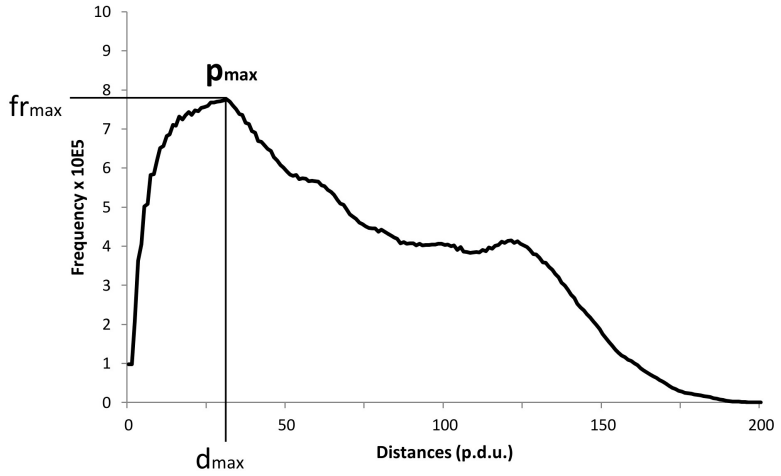

Thus we have two variables at our disposal for every graph: the distance (d_{max}) and the frequency (fr_{max}). The parameter d_{max} therefore represents the distance at the maximal frequency (fr_{max}). In order to seek out statistical differences among the various groups, we had to group all pertaining distances (d_{max}) and frequencies (fr_{max}) based on S_j or t_i. We designated the averages of these treatments as D_{max} and FR_{max}; for instance since there are three S_j we have three D_{max} values and three FR_{max} values (grouping triplets from all given incubation times—t_i).

3.5. Statistical Analysis

Results are expressed as average ± SE. The difference in each group was evaluated by one-way ANOVA (with Duncan's multiple range test) or Kruskal–Wallis test for non-normal distributed data. Linear regression by the least-squares method was carried out. All statistical tests were performed with Statgraphics Centurion XV (StatPoint Technologies, Warrenton, VA, USA). Value of $p < 0.05$ was considered as statistically significant.

4. Conclusions

In conclusion, we can say that the evaporation method with our special frequency analysis showed statistically significant differences in both: the incubation time domain (t_i) and the S/V-ratio domain (S_j), though they were more pronounced with FR_{max} than D_{max}. These results speak only about the differences of some water features when certain parameters (time, S/V-ratio) change, but they do not directly reveal any higher (supramolecular) order. The latter was found in an increasing dependence in the t_i domain, thus further corroborating the hypothesis of water self-ordering capacities that are at least partially covered by the term autothixotropy, researched by other methods—mechanical [19] and electrical conductivity measurements [21]. This further confirmation of the self-ordering nature of water (with ions) is not only important to physical chemistry, but—as stated by Vybiral [22]—it may be also very important for biology, since there are so many surfaces, especially on the subcellular level, that could influence water in the direction of increased (by resting) or decreased (by moving) orderliness. This investigation did not disclose any such increasing order depending on S/V-ratio, however, as already stated, our method was very limited and some other method could reveal some measure of self-ordering capacity also here, as it was discovered by Verdel *et al.* [21]. Further studies along this line should follow.

Author Contributions

Both authors have contributed equally to design of the study and preparation of the article. They have read and approved the final manuscript.

Conflicts of Interest

The authors declare no conflict of interest.

References and Notes

1 Ball, P. Water—an enduring mystery. *Nature* **2008**, *452*, 291–292.
2 Ho, M.W. Large supramolecular water clusters caught on camera—a review. *Water* **2014**, *6*, 1–12.
3 Chaplin, M.F. The memory of water: An overview. *Homeopathy* **2007**, *96*, 143–150.
4 Del Giudice, E.; Spinetti, P.R.; Tedeschi, A. Water dynamics at the root of metamorphosis in living organisms. *Water* **2010**, *2*, 566–86.
5 Zheng, J.M.; Chin, W.C.; Khijniak, E.; Khijniak, E., Jr.; Pollack, G.H. Surfaces and interfacial water: Evidence that hydrophilic surfaces have long-range impact. *Adv. Colloid Interface Sci.* **2006**, *127*, 19–27.
6 Yakhno, T.A.; Sedova, O.A.; Sanin, A.G.; Pelyushenko, A.S. On the existence of regular structures in liquid human blood serum (plasma) and phase transitions in the course of its drying. *Tech. Phys.* **2003**, *48*, 399–403.
7 Chen, G.; Mohamed, G.J. Complex protein patterns formation via salt-induced self-assembly and droplet evaporation. *Eur. Phys. J. E* **2010**, *33*, 19–26.

8 Kokornaczyk, M.O.; Dinelli, G.; Marotti, I.; Benedettelli, S.; Nani, D.; Betti, L. Self-organized crystallization patterns from evaporating droplets of common wheat grain leakages as a potential tool for quality analysis. *Sci. World J.* **2011**, *11*, 1712–1725.

9 Deegan, R.D. Pattern formation in drying drops. *Phys. Rev. E* **2000**, *61*, doi:10.1103/PhysRevE.61.475.

10 Weon, B.M.; Je, J.H. Self-pinning by colloids confined at a contact line. *Phys. Rev. Lett.* **2013**, *110*, 028303.

11 Deegan, R.D.; Bakajin, O.; Dupont, T.F.; Huber, G.; Nagel, S.R.; Witten, T.A. Capillary flow as the cause of ring stains from dried liquid drops. *Nature* **1997**, *389*, 827–829.

12 Deegan, R.D. Contact line deposits in an evaporating drop. *Phys. Rev. E* **2000**, *62*, 756–765.

13 Yakhno, T.; Yakhno, V.; Sanin, A.; Sanina, O.; Pelyushenko, A. dynamics of phase transitions in drying drops as an information parameter of liquid structure. *Nonlinear Dyn.* **2005**, *39*, 369–374.

14 Kokornaczyk, M.O.; Trebbi, G.; Dinelli, G.; Marotti, I.; Bregola, V.; Nani, D.; Borghini, F.; Betti, L. Droplet evaporation method as a new potential approach for highlighting the effectiveness of ultra high dilutions. *Complement. Ther. Med.* **2014**, *22*, 333–340.

15 Del Giudice, E.; Vitiello, G. Role of the electromagnetic field in the formation of domains in the process of symmetry-breaking phase transition. *Phys. Rev. A* **2006**, *74*, 022105.

16 Rey, L. Thermoluminescence of ultra-high dilutions of lithium chloride and sodium, chloride. *Physica A* **2003**, *323*, 67–74.

17 Rey, L. Can low-temperature thermoluminiscence cast light on the nature of ultra-high dilutions? *Homeopathy* **2007**, *96*, 170–174.

18 Pollack, G.H.; Figueroa, X.; Zhao, Q. Molecules, water, and radiant energy: New clues for the origin of life. *Int. J. Mol. Sci.* **2009**, *10*, 1419–1429.

19 Vybíral, B.; Voráček, P. Long term structural effects in water: Autothixotropy of water and its, hysteresis. *Homeopathy* **2007**, *96*, 18–188.

20 Verdel, N.; Jerman, I.; Bukovec, P. The "Autothixotropic" phenomenon of water and its role in proton transfer. *Int. J. Mol. Sci.* **2011**, *12*, 7481–7494.

21 Verdel, N.; Jerman, I.; Krasovec, R.; Bukovec, P.; Zupancic, M. Possible time-dependent effect of ions and hydrophilic surfaces on the electrical conductivity of aqueous solutions. *Int. J. Mol. Sci.* **2012**, *13*, 4048–4068.

22 Vybíral, B. Autothixotropy of water and its possible importance for the cytoskeletal structures. *J. Phys. Conf. Ser.* **2011**, *329*, 012004.

23 Yakhno, T.A. Surface properties of vitally important ions: Sessile desiccated drop studies. *Phys. Chem.* **2012**, *2*, 1–8.

24 Bevk, M.; Kononenko, I. A statistical approach to texture description of medical images: A preliminary study. In Proceedings of the 15th IEEE Symposium on Computer-Based Medical Systems (CBMS 2002), Maribor, Slovenia, 7 June 2002; pp. 239–244.

25 Kokornaczyk, M.O.; Dinelli, G.; Betti, L. Approximate bilateral symmetry in evaporation-induced polycrystalline structures from wheat grain leakages and fluctuating asymmetry as quality indicator. *Naturwissenschafften* **2013**, *100*, 111–115.

26 Kokornaczyk, M.O.; Parpinello, G.P.; Versari, A.; Rombolà, A.D.; Betti, L. Qualitative discrimination between organic and biodynamic Sangiovese red wines for authenticity. *Anal. Methods* **2014**, *6*, 7484–7488, doi: 10.1039/C4AY00971A
27 Ruth Kübler. Available online: http://www.ruthkuebler.org (accessed on 18 June 2014).
28 Wasser als Gedächtnis und Spiegel—The memory of water (in German). Available online: http://www.weltimtropfen.de (accessed on 18 June 2014).
29 Mikroskopische Wasseruntersuchungen. Available online: http://www.wasserstudio-bodensee.de/wasserstudio/mikroskopische-wasseruntersuchung (accessed on 18 June 2014).
30 Wasser-lebt. Available online: http://www.wasser-lebt.at (accessed on 18 June 2014).
31 Schröcker, G. The water world. *Science to Sage* Available online: http://issuu.com/sciencetosage/docs/dec_water_2012 (accessed on 18 June 2014).